energies

MDPI

Article

A Comparative Study on Load Assessment Methods for Offshore Wind Turbines Using a Simplified Method and OpenFAST Simulations

Satish Jawalageri [1,2,*], Subhamoy Bhattacharya [3], Soroosh Jalilvand [2] and Abdollah Malekjafarian [1,*]

[1] Structural Dynamics and Assessment Laboratory, School of Civil Engineering, University College Dublin, D04 V1W8 Dublin, Ireland
[2] Gavin and Doherty Geosolutions, D14 X627 Dublin, Ireland; soroosh@gdgeo.com
[3] Department of Civil and Environmental Engineering, University of Surrey, Guildford GU2 7XH, UK; s.bhattacharya@surrey.ac.uk
* Correspondence: satish.jawalageri@ucdconnect.ie (S.J.); abdollah.malekjafarian@ucd.ie (A.M.)

Abstract: Simplified methods are often used for load estimations during the initial design of the foundations of offshore wind turbines (OWTs). However, the reliability of simplified methods for designing different OWTs needs to be studied. This paper provides a comparative study to evaluate the reliability of simplified approaches. The foundation loads are calculated for OWTs at the mudline level using a simplified approach and OpenFAST simulations and compared. Three OWTs, NREL 5 MW, DTU 10 MW, and IEA 15 MW, are used as reference models. An Extreme Turbulence Model wind load at a rated wind speed, combined with a 50-year Extreme Wave Height (EWH) and Extreme Operating Gust (EOG) wind load and a 1-year maximum wave height are used as the load combinations in this study. In addition, the extreme loads are calculated using both approaches for various metocean data from five different wind farms. Further, the pile penetration lengths calculated using the mudline loads via two methods are compared. The results show that the simplified method provides conservative results for the estimated loads compared to the OpenFAST results, where the extent of conservativism is studied. For example, the bending moment and shear force at the mudline using the simplified approach are 23% to 69% and 32% to 53% higher compared to the OpenFAST results, respectively. In addition, the results show that the simplified approach can be effectively used during the initial phases of monopile foundation design by using factors such as 1.5 and 2 for the shear force and bending moment, respectively.

Keywords: offshore wind turbines; monopile; simplified method; Ultimate Limit State (ULS); OpenFAST

check for updates

Citation: Jawalageri, S.; Bhattacharya, S.; Jalilvand, S.; Malekjafarian, A. A Comparative Study on Load Assessment Methods for Offshore Wind Turbines Using a Simplified Method and OpenFAST Simulations. *Energies* **2024**, *17*, 2189. https://doi.org/10.3390/en17092189

Academic Editor: Mehdi Shokouhian

Received: 25 March 2024
Revised: 23 April 2024
Accepted: 25 April 2024
Published: 2 May 2024

Copyright: © 2024 by the authors. Licensee MDPI, Basel, Switzerland. This article is an open access article distributed under the terms and conditions of the Creative Commons Attribution (CC BY) license (https://creativecommons.org/licenses/by/4.0/).

1. Introduction

In recent years, the wind energy sector has undergone a rapid expansion due to its demonstrated potential as a leading and reliable source of renewable energy. OWTs are considered to be more effective than onshore wind turbines, where the wind speed and its direction are more consistent, resulting in higher energy resources to be exploited. As a consequence, there has been a substantial increase in investments directed towards this sector in recent years. For example, there will be around 25 GW of offshore wind capacity installed in Europe by the end of 2020, with further plans to expand this to around 85 GW over the following decade [1].

Foundations are important components of OWTs and need to be installed in the seabed. There are several foundation types for OWTs, such as monopile, jacket, gravity-based, etc. Figure 1 shows the cumulative number of each foundation type installed by the end of 2020 in the world. It shows that the monopile foundation is the most common type of foundation installed (81.2%) [1,2]. This is mostly due to its simple design compared to

other options and its suitability for the mass fabrication and mass installation of such foundations [3]. In addition, turbine technology is rapidly evolving, which has resulted in more advanced wind turbines with higher capacities and larger sizes. By increasing the size of the structure and OWTs, the aerodynamic and hydrodynamic loads on the structure will be higher, which results in higher deflection and rotation of the monopile at the mudline level [4]. This means that there is also a need for more advanced foundations that can carry higher loadings, potentially with larger diameters. For example, the current monopiles being installed for OWTs are in the diameter range of 8 m to 10 m or beyond [5].

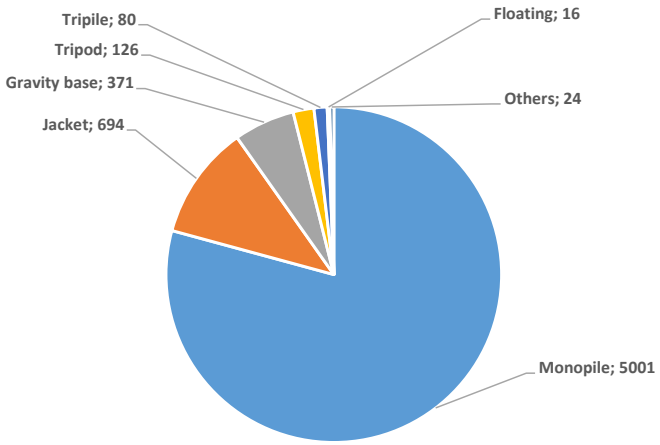

Figure 1. Number of foundation types up to 2022 [6].

The increase in loads acting on the OWT structure due to the use of a larger turbine size would result in higher pile penetration lengths depending on the soil conditions. For monopile design, a load assessment needs to be carried out, which consists of calculating the loads at the mudline level. This includes assessing the wind and wave loads on the structure, while soil condition requires site-specific soil characteristics from the depth below the mudline. For example, Krolis and Zwaag [7] investigated the change in pile diameter and soil conditions with pile embedment for smaller turbines. They showed that the pile penetration length varies with varying soil conditions. In addition, OWTs are exposed to harsh environmental conditions, which could be a threat to their structural integrity [8,9]. The presence of scour erosion around the monopile foundation is one of the main issues with OWTs. This means that soil material is removed around the monopile due to the actions of currents, tides, and waves. Therefore, it should be highlighted that monopiles are highly sensitive to scour occurrence, which could result in strength and stiffness reductions in these foundations [10,11]. On the other hand, the sea surface will have an impact on offshore wind turbine performance. Wu, et al. [12] studied how ocean–atmosphere interactions influence offshore wind farm performance using a coupled simulation method. The results indicate that offshore wind farm wakes disperse more rapidly over the ocean, reducing the power output of downwind turbines by 10% and reducing the wind power by 3.5% due to the increased wind shear from ocean waves. In addition, Pettas, et al. [13] investigated how the presence of multiple offshore wind farms at varying distances affects wind conditions and turbine performance at Alpha Ventus. Their findings highlight reduced wind speeds, increased turbulence, and higher turbine loads due to inter-farm interactions.

In addition to mudline loads and soil conditions, the calculation of the pile embedment length also depends on the natural frequency of the system. In general, it is recommended that the natural frequency of the system avoid excitation frequencies such as the frequencies caused by waves and wind and the frequencies corresponding to the rotational speed of the turbine (1P and 3P); 1P is the frequency referring to the operating range of the wind turbine, and 3P represents the loads that the tower is subjected to, due to the shadowing effect of blades [14]. Figure 2 illustrates the power spectral density (PSD) of typical waves and winds, along with 1P and 3P frequency ranges, which depend on the rotor frequency.

The figure also shows the different potential design types for OWTs: namely, soft–soft, soft–stiff, and stiff–stiff. In general, the first global natural frequency (i.e., the first frequency of the complete wind turbine structure, including the rotor, nacelle assembly, WTG tower, and substructure) will lie in the range of 1P plus a safety margin and 3P plus a safety margin, where the design is soft–stiff, and this is common practice in the current offshore industry. However, for the soft–soft design, the natural frequency is below 1P, which results in a very flexible and impractical design for fixed-base OWTs. On the other hand, the stiff–stiff design is the option where the natural frequency of the system is beyond the 3P frequency, requiring a very stiff support structure [14]. In addition, the natural frequency of the system is dependent on the structural mass and stiffness of the coupled system, which need to be obtained from the geometry of the system and soil conditions. For example, Jacomet, et al. [15] investigated the influence of monopile embedment length on the natural frequency and tower displacement. They showed that the natural frequency decreases with a decrease in embedment length, which eventually increases the displacement of the tower.

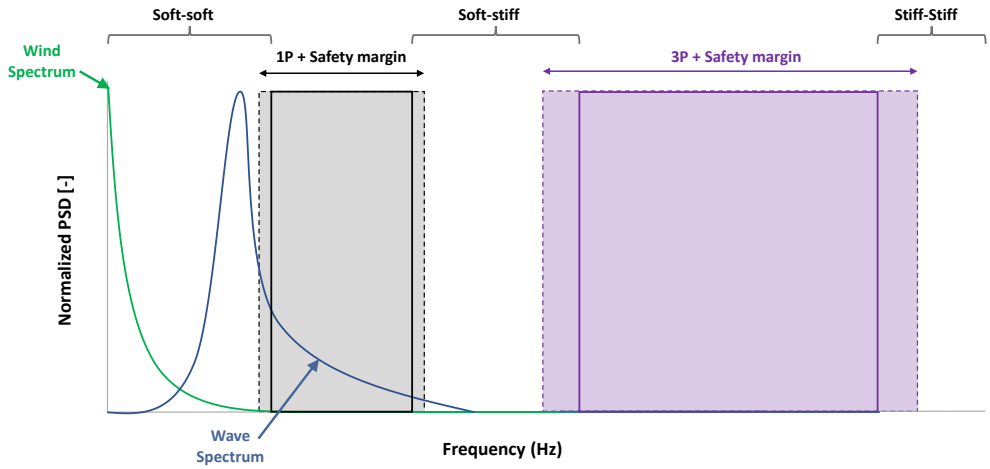

Figure 2. Various ranges of wind turbine frequencies (modified after [14]).

To ensure the feasibility of power generation from offshore wind, it is crucial to optimize the design of offshore substructures for cost-effectiveness [16]. This may be achieved by reducing the uncertainties in the calculation of the environmental loads acting on these structures. In addition, to ensure the structural safety of OWTs through their lifetime, the maximum loads, i.e., the ultimate loads subjected to the monopiles, must be assessed [17]. The main function of the monopiles is to safely transfer all the loads from the top of the structure to the mudline during its design life and to resist allowable deformations. The design load calculations should ensure that the chosen foundation can effectively resist the maximum ultimate and fatigue loads acting on the structure throughout its operational lifetime [14]. However, the combination of hydrodynamic, aerodynamic, non-linear interactions between the soil and the structure and the effect of the controller makes monopile design a very challenging process [18]. In recent years, several detailed mathematical models including hydrodynamics, aerodynamics, and servo dynamics have been developed for OWTs (such as Bladed v4.15, HAWC2 v13.0.5, SIMA v4.24.2, Orcaflex v11.4, OpenFAST v3.5.3, etc.) to assess the influence of these parameters on the dynamics of a structure. Although these models have the potential to provide more accurate and reliable solutions in terms of load assessment for OWTs, the high level of complexity makes them computationally expensive for these types of analysis [19].

There have been several studies in recent years on quantifying the critical parameters for load assessment in OWTs. Jeong, et al. [20] investigated the impact of wave loads on OWTs' structures. Their study focused on three types of offshore support structures: namely, monopile, gravity-based, and jacket structures. They found that the wave forces tend to increase with an increase in the diameter of the structure. This information provides insights

into how wave loads can affect the structural integrity and stability of OWTs. On the other hand, wind loads play a critical role in the design of OWTs. As shown in a comparative study by [21], the impact of the wind load on the monopile structure can be noteworthy, potentially leading to a contribution of up to 50% in horizontal residual displacement and maximum bending moment. Therefore, considering the dynamic influence of both hydrodynamic loads (such as wave-induced loads) and aerodynamic loads (such as wind loads) is crucial in understanding and predicting the behaviour of OWT structures [22–24]. These loads can have significant impacts on the structural response, including deformations, stresses, and fatigue, which can affect the overall performance, safety, and durability of the OWT [25–27]. Therefore, a comprehensive understanding and consideration of both types of loads are essential in the design, analysis, and operation of OWT structures to ensure their safe and efficient performance over their intended service life.

In general, OWTs are designed for a lifetime of 25–30 years. OWT foundations are designed using a complex process based on the site characteristics and turbine size, which will result in the dimensions and geometry of the foundation. The design load cases (DLCs) provided in the standards [28,29] are normally used to assess the OWT in different loading conditions. The design process is normally carried out in two phases: conceptual design and detailed design. The details and accuracy needed for the OWT model differ from the conceptual design stage to the detailed design stage. However, the foundation designers normally change the turbine type and its dimensions several times during the conceptual phase of a project. This means that the conceptual design process needs to be repeated several times, which will be extremely time-consuming if a complex model is used. Therefore, several studies have suggested that having a simplified design approach during the conceptual design of a monopile foundation could be very beneficial.

There are many studies that provide insights into various frameworks to be used in the conceptual and detailed design of offshore foundation structures [30–32]. However, there are limited studies regarding simplified methods to obtain the loads and design the offshore foundation structures during the conceptual design phase. Ishwarya, et al. [33] proposed a simplified procedure for designing monopile foundation structures for OWTs. They demonstrated that using simplified equations for determining the monopile diameter and pile length can be beneficial in the preliminary design of offshore monopile foundations in wind turbine projects. Yang, et al. [34] proposed a simplified method for estimating the fundamental frequency of monopile foundations for design purposes. Ma, et al. [35] proposed a simplified method for analysing the permanent accumulated rotation of monopile foundations during the design process. In addition, Li, et al. [36] estimated the initial stiffness of monopile foundations for OWTs. They proposed a simplified method that could estimate the mechanical behaviour of monopiles under later loads at the interface level. Arany, et al. [37] introduced a simplified design approach for designing monopiles in 10 steps. It included the calculation of wind and wave loads based on the turbine specifications and site-specific metocean data. They proposed two load combinations that were more conservative to calculate the ultimate loads for a simplified approach, namely: (i) the Extreme Turbulence Model (ETM) wind load at the rated wind speed combined with the 50-year Extreme Wave Height (EWH) and (ii) the Extreme Operating Gust (EOG) wind load combined with the 1-year maximum wave height. The mudline design loads can be obtained from this method and can eventually be used to determine the design parameters of monopile foundations, such as the pile dimensions and embedment length.

Foundation design for OWTs is known as an iterative process due to load iterations. This means that the foundation stiffness is required for aero–servo–hydro simulations that generate the turbine loads that are experienced by the foundation. Furthermore, foundation stiffness is dependent on the turbine size and needs to be estimated before the simulations. As discussed above, simplified methods can be used for load estimations during the initial design stage. However, the reliability of simplified methods for designing different OWTs is not yet clear and needs to be studied. This means that their reliability needs to be checked

against the results from a more complex model with higher fidelity. In addition, such a study should be extended to different turbine sizes.

To address the challenges mentioned above, for the first time in the literature, a comparison study is carried out to assess the reliability of simplified approaches in predicting the loads on wind turbines. The simplified approach previously proposed by [37] is employed for the design. The loads calculated using the simplified approach are compared to the results obtained from OpenFAST simulations for three different wind turbines supported on monopile foundations, including the largest reference turbine available (NREL 15 MW). In addition, a comparison of the extreme loads between the simplified and OpenFAST methods is carried out for various metocean parameters, which may include factors such as wave height, water depth, and other relevant environmental conditions. Furthermore, the pile penetration length is calculated based on medium-dense sand and mudline loads obtained from both the simplified approach and OpenFAST software. In addition, for the first time, scaling factors are defined, allowing us to use simplified methods with higher levels of reliability in future studies. The results of this study may be of interest in the initial stage of OWT design and can potentially guide the industry on the effective use of simplified approaches.

2. Theoretical Background

2.1. Loads Acting on OWTs

This section introduces various external loads acting on the OWTs. In addition to the self-weight of the structure, there are four primary loads acting on OWTs: namely, (a) wind (aerodynamic load), (b) waves (hydrodynamic load), (c) 1P load (rotor frequency), and (d) 3P load (blade-passing frequency) [14]. Figure 3 shows the various loads experienced by the wind turbine during the service time of the structure.

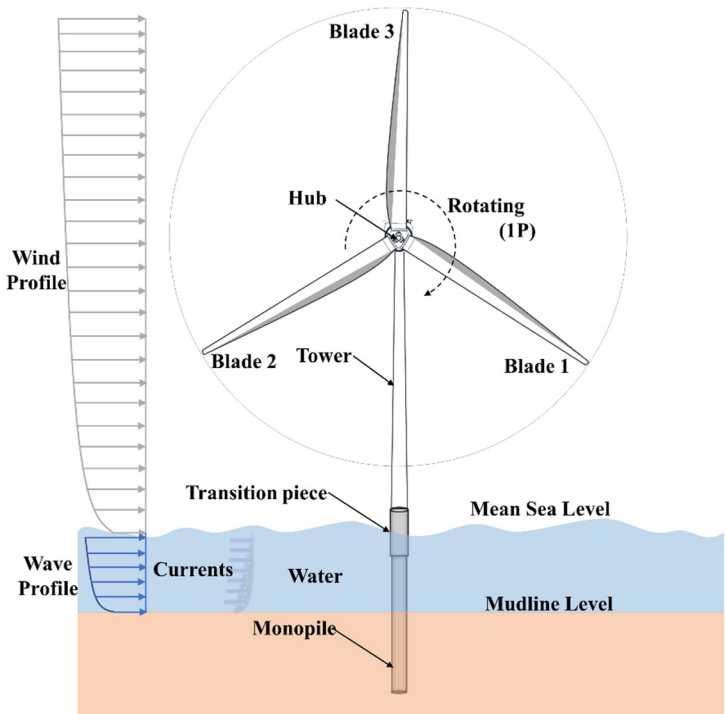

Figure 3. Loading on fixed offshore wind turbine atop monopile.

Aerodynamic loads are caused due to the wind acting on the structure. These loads are produced by the thrust of the wind subjected to the tower and blades. These loads are normally calculated based on the wind characteristics at the site and wind turbine generator (WTG) characteristics. The loads at the interface level will be higher if the hub height of the turbine is at a higher level.

Hydrodynamic loads are caused due to the water waves acting on the substructure of OWTs (i.e., part of the structure submerged in water). These wave loads depend on site-specific characteristics such as the wave height and wave period, along with the water depth. In addition, the magnitude of wave loads depends on the diameter of the substructure; i.e., the higher the diameter, the higher the magnitude of the load at the mudline level.

The 1P load is a load caused due to the vibration of the rotor at the hub-height level because of the mass and aerodynamic imbalance of the rotor, which corresponds to the rotational frequency of the rotor. This frequency varies according to the turbine characteristics, i.e., the cut-in and rated revolutions per minute (rpm). Hence, 1P will result in the range between the highest and lowest rpm. However, the design of the structure should not be in these frequency ranges, to avoid resonance.

The 3P loads, also referred to as blade-passing loads, are the loads on the tower due to the vibration caused by the shadowing effect of blades; i.e., there will be changes in the load acting on the tower when the blade passes through the front of the tower (reducing the thrust on the tower). In addition, the loads are heavily influenced by the rotational speed of the rotor under turbulent fields. This effect depends on the number of blades, and its frequency can be obtained by multiplying the number of blades by the rotor frequency (1P).

2.2. A Simplified Approach to Load Calculation

This section introduces a simplified method to calculate the ultimate loads at the mudline for OWTs including wind and wave loads, as proposed by [37]. Two load combinations are chosen to find out the ultimate loads. Wind loads are calculated for the Extreme Turbulence Model (*ETM*) at the rated wind speed and the 50-year Extreme Operating Gust (*EOG*), and are used in the Ultimate Limit State (ULS) load combinations. Wind loads corresponding to the ETM at the rated wind speed use the standard deviation of wind speed at the rated wind speed, while the EOG uses a long-term distribution of 10 min mean wind speeds.

The standard deviation of the wind speed in the ETM ($\sigma_{u,ETM}$) is given in [38], as follows:

$$\sigma_{u,ETM} = cI_{ref}\left[0.072\left(\frac{U_{avg}}{c}+3\right)\left(\frac{U_R}{c}-4\right)+10\right] \tag{1}$$

where c is a constant of 2 m/s, I_{ref} represents the reference turbulence intensity depending on the turbine class, U_{avg} is the long-term average wind speed at the site, and U_R is the rated wind speed.

The maximum turbulent wind speed component u_{ETM} is determined as follows [37]:

$$\sigma_{u,ETM,f>f_{1P}} = \sigma_{u,ETM}\sqrt{\frac{1}{\left(\frac{6L_k}{U_R}f_{1P,max}+1\right)^{\frac{2}{3}}}} \tag{2}$$

where L_k is the integral length scale and $f_{1P,max}$ is the rotational speed of the turbine.

The turbulent wind speed is calculated as follows:

$$u_{ETM} = 2\sigma_{u,ETM,f>f_{1P}} \tag{3}$$

The ultimate loads corresponding to the ETM are as follows:

$$F_{wind,ETM} = \frac{1}{2}\rho_a A_R C_T\left(U_R+u_{ETM}\right)^2 \tag{4}$$

$$M_{wind,ETM} = F_{wind,ETM}\left(S+z_{hub}\right) \tag{5}$$

where $F_{wind,ETM}$ and $M_{wind,ETM}$ are the lateral force and moment at the mudline level, ρ_a is the density of air, A_R is the rotor-swept area, C_T is the thrust coefficient, S represents the water depth, and z_{hub} is the hub height above sea level.

The maximum force is assumed to occur when the maximum mean thrust force acts and the 50-year Extreme Operating Gust (*EOG*) hits the rotor. Due to this sudden gust, the wind speed is assumed to change so fast that the pitch control does not have time to adjust the blade pitch angles. This assumption is very conservative, as the pitch control, in reality, has a time constant, which would allow for some adjustment to the blade pitch.

The wind load corresponding to the *EOG* is calculated as follows:

$$F_{wind,EOG} = \frac{1}{2}\rho_a A_R C_T (U_R + u_{EOG})^2 \tag{6}$$

$$M_{wind,EOG} = F_{wind,EOG}\,(S + z_{hub}) \tag{7}$$

where $F_{wind,EOG}$ and $M_{wind,EOG}$ are the lateral force and moment at the mudline level corresponding to the *EOG* condition and u_{EOG} is the maximum wind speed component of the EOG condition.

The simplified approach uses Morison's equation in order to calculate the wave loads on the structure. It should be noted that Morison's equation can be used when the wavelength is greater than 5 times the diameter of the monopile [39]. It uses the 50-year wave period and wave height to calculate the load. The extreme wave height corresponding to return periods of 1 year (H_1) and 50 year (H_{m}) is calculated using the following formula [37]:

$$H_{S,1} = 0.8 H_{S,50} \tag{8}$$

$$T_{S,1} = 11.1\sqrt{\frac{H_{S,1}}{g}} \tag{9}$$

$$H_1 = H_{S,1}\sqrt{\frac{1}{2} ln\left(\frac{10800}{T_{S,1}}\right)} \tag{10}$$

$$T_1 = 11.1\sqrt{\frac{H_1}{g}} \tag{11}$$

$$H_{\mathrm{m}} = H_{S,50}\sqrt{\frac{1}{2} ln\left(\frac{10800}{T_S}\right)} \tag{12}$$

$$T_m = 11.1\sqrt{\frac{H_m}{g}} \tag{13}$$

where $H_{S,50}$ is the extreme wave height corresponding to the return period of 50 years, $T_{S,1}$ is the time period corresponding to the return period of 1 year, and H_1 and T_1 are the wave height and wave period for the 1-year return period, respectively.

To obtain foundation loads in the simplified method, it can be conservatively assumed that the design wave load is the sum of the maxima of drag and inertia loads. This assumption is conservative, because the maxima of the drag load and inertia load occur at different time instants. Therefore, wave loads are calculated based on the above calculated values, as follows [37]:

$$F_{D,max} = \frac{1}{2}\rho_w D_s C_D \frac{\pi^2 H^2}{T^2 \sin h^2(kS)}\, P_D(k, S, \eta) \tag{14}$$

$$M_{D,max} = \frac{1}{2}\rho_w D_s C_D \frac{\pi^2 H^2}{T^2 \sin h(kS)}\, Q_D(k, S, \eta) \tag{15}$$

where,

$$P_I(k, s, \eta) = \frac{\sin h(k(S + \eta))}{k} \text{ and} \tag{16}$$

$$Q_I(k,s,\eta) = \left(\frac{S+\eta}{2k} - \frac{1}{2k^2}\right)e^{k(S+\eta)} - \left(\frac{S+\eta}{2k} + \frac{1}{2k^2}\right)e^{-k(S+\eta)} + \frac{1}{k^2} \quad (17)$$

where $F_{D,max}$ and $F_{I,max}$ are the maximum drag and inertia forces, $M_{D,max}$ and $M_{I,max}$ are the maximum drag and inertia moments, ρ_w is the density of water, D_s is the diameter of the substructure, C_D and C_m are the drag and inertia coefficients, H and T are the wave height and period where H_m and T_m are used for the calculation of the 50 year wave load, respectively, and H_1 and T_1 are used for 1 year wave load calculations, and k is the wave number where $k = 2\pi/\lambda$, λ is the wave length, S is the water depth, and η is the surface elevation.

The total wave load is calculated as follows:

$$F_{wave} = F_{D,max} + F_{I,max} \quad (18)$$

$$M_{wave} = M_{D,max} + M_{I,max} \quad (19)$$

3. Methodology: Load Estimation Using OpenFAST Simulations

This section illustrates the methodology behind OpenFAST software and the various modules that we used. OpenFAST is an open source aero–hydro–servo–elastic software. The main modules in OpenFAST are SubDyn v1.01 and ElastoDyn v1.00 for modelling structural dynamics, ServoDyn v1.05 for modelling power generation, and InflowWind v3.01, HydroDyn v2.03, and AeroDyn v15 for modelling the external wind conditions, hydrodynamic properties, and aerodynamics of the system, respectively. It should be noted that the stiffness of the monopile is modelled in OpenFAST by providing the monopile dimensions. However, the stiffness of the monopile below the mudline is ignored, as the rigid or fixed foundation has been considered.

3.1. Wind Loads

The wind loads acting on the structure represent the dominant load during the operation of OWTs. The turbine tower and blades are subjected to the wind loads acting on the wind turbines. OpenFAST uses blade element momentum (BEM) theory [40] to calculate the aerodynamic loadings on the location along the blades. BEM theory is the combination of blade element theory (or propeller theory) and momentum theory. Blade element theory calculates the forces by dividing the blade into a number of segments along the length, and then the force is calculated for each segment. Momentum theory incurs a reduction in velocity when wind passes through the rotor. BEM uses these two concepts to find the axial forces and torque acting on the rotor blades. Aerodyn is the module in OpenFAST that performs the aerodynamic simulations. Aerodyn calculates the drag, lift, and pitching moment of airfoil sections along the length of the turbine blade by dividing the blade into a number of segments. In addition, it calculates the forces for each segment with the use of the turbine geometry, operating conditions, blade-element velocity and location, and wind inflow, which are then used to calculate the forces along the blades. In this study, turbsim is used to generate the wind inflow where the reference wind speed is considered as 11.4 m/s for NREL 5 MW and DTU 10 MW at 10.59 m/s for IEA 15 MW, which is the rated wind speed for the respective considered turbine size. Turbsim is a standalone wind simulator that generates the three-dimensional wind velocity, along with the time-varying wind speeds.

In addition, the power law is used to calculate the wind load along the turbine tower as the wind speed along the vertical height changes [41]:

$$V(z) = V_{hub}\left(\frac{z}{z_{hub}}\right)^{\beta} \quad (20)$$

where $V(z)$ and V_{hub} are the mean wind speed at the height z above the MSL and *hub* height, z_{hub}, respectively, and the power law coefficient, β, of 0.143 has been considered in this study [14].

3.2. Wave Loads

Hydrodyn is a module in OpenFAST that is used to calculate hydrodynamic loads [42]. Figure 4 shows an overview of the wave parameters involved in the calculation of the wave loads on the structure. Linear regular waves have been considered for the calculation of hydrodynamic loads on the structure in this study. The hydrodynamic loads on the structure are calculated based on strip theory, using Morison's equation [43]. Morison's equation is a function of water particle velocity and acceleration along the depth, and the force per unit length along the cylinder is given by

$$dF_h = 0.5\,\rho_w\,C_d\,D\,dz\,|v_r|v_r\;+\;(C_m-1)\,\rho_w\,A(z)dz\,a_r \tag{21}$$

where ρ_w represents the density of water, $D\,dz$ is the area of the strip with the diameter (D) and, $A(z)dz$ is the displaced volume, v_r is the relative water velocity with respect to the velocity of the body, and a_r represents the relative fluid acceleration. In this study, wave kinematics (wave velocity and acceleration) along the depth are calculated from the seabed to the still-water level (SWL) without considering wave stretching, in order to estimate the wave loads along the monopile structure. Further, we used a wave period and wave height of 11.54 s and 10.6 m for the ETM load conditions, and a wave period and wave height of 10.49 s and 8.76 m for the EOG load condition, respectively.

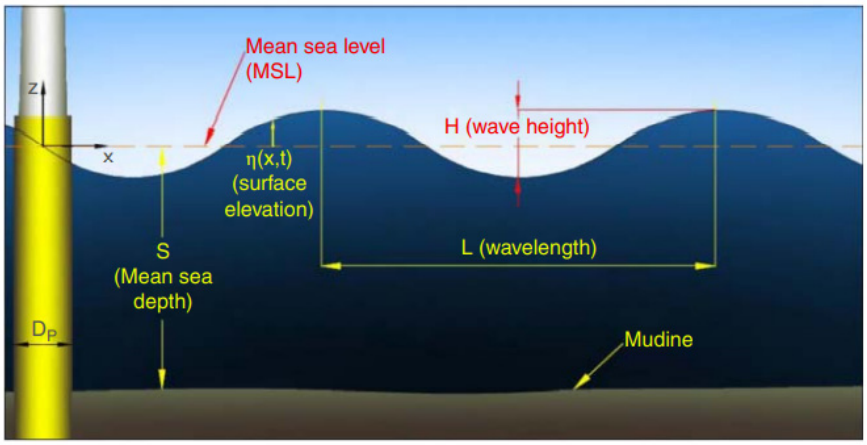

Figure 4. Overview of wave parameters [14].

3.3. Substructure

Subdyn is a module in OpenFAST that supports different substructure types, such as monopile, jackets, tripods, and other fixed structures. It allows the substructure to be modelled with a rigid bottom or the option of providing the stiffness matrix at the mudline level. This is to account for soil–structure interaction at the substructure interface level, which is rigidly connected to the transition piece. In this study, a monopile substructure clamped at the seabed is considered, to investigate the mudline loads under ULS conditions. Loads and responses are transferred at the interface between Subdyn, Hydrodyn, and Elastodyn (where the tower is modelled) to enable the hydro-elastic interaction at each time step [44].

3.4. Tower

ElastoDyn is a structural dynamics module within the OpenFAST software, used to model the tower and platform of wind turbines. It requires input files containing information on parameters such as degrees of freedom, initial conditions, and turbine configuration, including tower distributed properties and assumed mode shapes. Mode shapes, which are obtained outside of OpenFAST using software such as BModes v3.00, are specified as polynomial coefficients in the ElastoDyn file [45].

3.5. Servo System

ServoDyn is the control and electrical-drive module. It includes control and electrical-drive models for blade pitch, generator torque, nacelle yaw, high-speed shaft brake, and blade-tip brakes. Bladed-style dynamic link library (DLL) is one of the blade pitch control modes in OpenFAST and is considered as part of this study. A more detailed description of ServoDyn can be found in [45].

4. Results

This section presents the results for the mudline loads and pile penetration lengths for NREL 5 MW, DTU 10 MW, and IEA 15 MW turbines supported on the monopile offshore foundation. For each turbine size, the loads are calculated using the OpenFAST simulations with a total simulation time of 600 s where the extreme loads are extracted by considering the maximum load over the simulation time after the transient time of 30 s.

Jalbi, et al. [46] investigated the problem by focusing on the SLS criteria (i.e., long-term tilt) due to one-way/two-way loading owing to the combination of wind and wave. Numerous load cases are provided in the DNV, as well as the IEC codes for the design of offshore wind turbines to serve a service life of 25–30 years; however, only a few are relevant to foundation design, as discussed in [37] and shown in Table 1.

Table 1. Load scenarios are chosen for this study.

Name	Wind Model	Wave Model
Normal Operational Conditions	Normal Turbulence Model (NTM) at the rated wind speed (U_R)	1-Year Extreme Sea State (ESS)
Extreme Wave Load Scenario	Extreme Turbulence Model (ETM) at the rated wind speed (U_R)	50-Year Extreme Wave Height (EWH)
Extreme Wind Load Scenario	Extreme Operating Gust (EOG) at the rated wind speed (U_R)	1-Year Extreme Wave Height (EWH)

The two load combinations provided in the literature [37] are used in our analysis and are based on the ETM and EOG for the wind model. The metocean data used for the analysis are described in Sections 3.1 and 3.2. Further, two key parameters, mudline shear force and bending moment from each load combination, are used to compare the two methods.

4.1. Wind Turbine Models

This section introduces various Wind Turbine Generators (WTGs) used for the comparison of load estimated by OpenFAST and a simplified approach. In this study, three offshore wind turbines, namely, NREL 5 MW [47], DTU 10 MW [48], and IEA 15 MW [49] are considered as the base models. Table 2 shows the various parameters of three WTGs. The hub heights for 5 MW, 10 MW, and 15 MW are 90 m, 119 m, and 150 m, respectively, while the rotor diameters are 126 m, 178.3 m, and 240 m.

4.2. Comparison between the Simplified Approach and OpenFAST

Table 3 compares the mudline shear forces and bending moments calculated using the simplified approach and OpenFAST simulations for NREL 5 MW, DTU 10 MW, and IEA 15 MW turbines. It also gives the percentage error between the results obtained using two approaches. The percentage difference between the simplified and OpenFAST approaches is calculated as follows:

$$Percentage\ difference = \left| \frac{V_{OpenFAST} - V_{Simplified}}{V_{Simplified}} \right| \times 100 \quad (22)$$

where $V_{OpenFAST}$ represents the loads from OpenFAST and $V_{Simplified}$ represents the loads obtained from the simplified method.

Table 2. Properties of WTGs.

Parameter	Units	Value		
Power Rating	MW	5	10	15
Configuration	No.	3	3	3
Rotor, hub diameter	m	126, 3	178.3, 5.6	240, 7.94
Hub height	m	90	119	150
Rated rotor speed	rpm	12.1	9.6	7.56
Rotor mass	kg	110,000	229,000	144,962
Nacelle mass	kg	240,000	446,000	530,888
Tower mass	kg	347,500	605,000	860,000
MP diameter, wall thicknesses (above mudline)	m	6.0, 0.060	8.3, 0.060	10, 0.055
Tower top diameter, wall thickness	m	3.87, 0.019	5.5, 0.020	6.5, 0.024
Tower base diameter, wall thickness	m	6.0, 0.027	8.3, 0.038	10.0, 0.041

Table 3. Comparison of mudline loads from Simplified and OpenFAST results.

Turbine	Method	ETM with 50 Year EWH		EOG with 1 Year EWH	
		Shear Force (MN)	Bending Moment (MN·m)	Shear Force (MN)	Bending Moment (MN·m)
NREL 5 MW	Simplified Method	5.54	215.83	6.45	374.05
	OpenFAST	4.36	165.65	4.33	227.61
	Difference	21.28%	23.25%	32.92%	39.15%
DTU 10 MW	Simplified Method	10.07	507.32	11.65	850.36
	OpenFAST	6.24	154.98	5.39	166.32
	Difference	38.03%	69.45%	53.70%	80.44%
IEA 15 MW	Simplified Method	16.49	1073.14	19.16	1823.80
	OpenFAST	13.74	757.22	11.90	920.43
	Difference	16.66%	29.44%	37.89%	49.53%

The differences are listed in Table 3, and they are also shown in Figures 5 and 6. It can be seen that shear forces and bending moments increase with an increase in turbine size, as there is a change in structural geometry and rotor diameter. For instance, the bending moment obtained from the simplified approach corresponding to the ETM with 50 year EWH resulted in 215.8 MN·m and 1073.1 MN·m for the NREL 5 MW and IEA 15 MW turbine, respectively. Furthermore, it can be observed that the simplified method provides larger values for all turbine sizes compared to the OpenFAST results. For example, for an EOG with a 1-year EWH, using the simplified method for the NREL 5 MW turbine, results in errors of 32.9% and 39.2% for the shear force and bending moment compared to OpenFAST, respectively. Similarly, the simplified approach provides 37.9% and 49.5% higher values for the shear force and bending moment for IEA 15 MW compared to OpenFAST for the EOG with 1 year EWH. These higher values for the simplified method are due to the conservatism considered in its approach [37]. However, it is necessary to consider a number of case studies in order to validate the results between two methods, and this is illustrated in the next section. It should also be noted that the differences between the loads calculated using both methods are relatively larger in the case of the DTU 10 MW OWT. This could be due to factors such as the model complexity, calibration variations, lack of validation, and higher sensitivity to the assumptions.

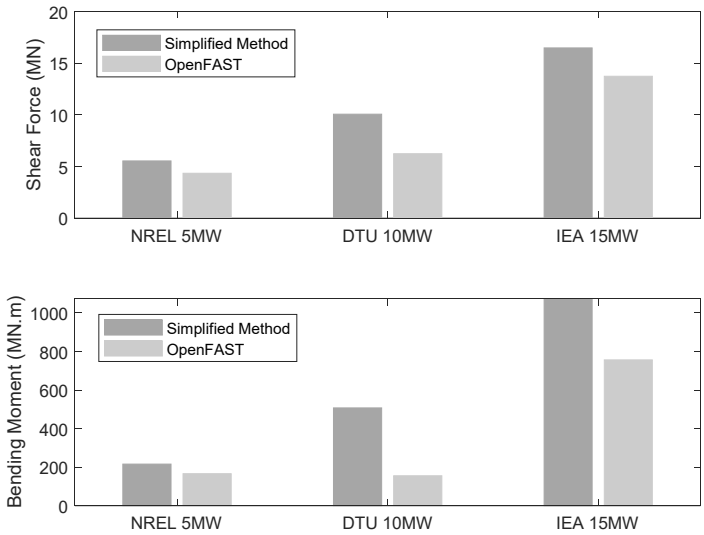

Figure 5. Comparison of loads corresponding to ETM with 50 year EWH: shear force (**top**) and bending moment (**bottom**).

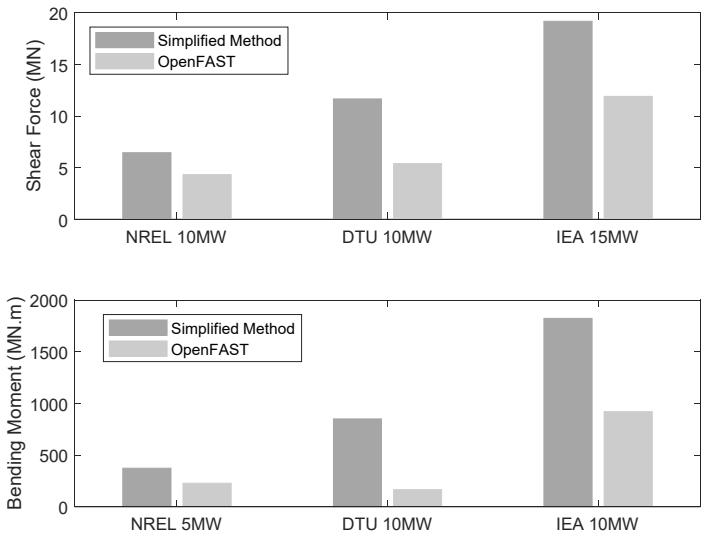

Figure 6. Comparison of loads of corresponding to EOG with 1 year EWH: shear force (**top**) and bending moment (**bottom**).

The results highlight a clear relationship between the size of the turbine and the corresponding magnitudes of loads experienced by the structure, whereby an increase in turbine dimensions is associated with a corresponding increase in the imposed loads. This means that an increase in environmental loads acting on OWT structures can have a significant impact on the steel utilizations for the structure. The steel utilizations of the structure refer to the extent to which the steel materials in the structure are being used or stressed relative to their design capacities. With higher environmental loads, the steel utilization may increase, which means that the steel components of the OWT structure may be approaching or exceeding their design capacities. The structural components of the OWT systems may experience higher stresses, deformations, and fatigue effects due to the increase in the loads acting on them [50]. This can result in additional steel reinforcement or thicker sections to ensure that the structure can withstand the increased loads without excessive deformations or structural failures.

Further, as mudline loads increase, it may be necessary to increase the pile penetration length to ensure that the foundation can withstand the higher loads. The pile penetration plays a crucial role in providing sufficient stability, bearing capacity, and resistance against

uplift, lateral, and cyclic loads for the monopile foundation [3,51]. It is important to accurately assess and account for mudline loads and their impact on the pile penetration length during the design of offshore wind turbine foundations to ensure the safe and reliable operation of the structure throughout its expected service life. In this study, a comparison of pile penetration lengths is performed based on different metocean parameters and is described in Section 4.4.

4.3. Site-Specific Loads Using a Simplified Approach and OpenFAST

This section introduces the analysis of extreme loads calculated using the simplified and OpenFAST method for various metocean data from different wind farms. Five wind farms, namely, 'Barrow II', 'Belwind IV', 'Walney I', 'London Array 1', and 'Thanet III', are considered [46]. Table 4 shows the summary of metocean data for various wind farms used for the analysis where the average water depth across the considered wind farms is approximately 22 m. In addition, Barrow II has a lower H_s and T_p with a return period of 50 years of 7.5 m and 9.7 s, respectively, increasing up to H_s of 10.5 m and T_p of 11.9 s for Thanet III, respectively.

Table 4. Metocean data from wind farms.

Wind Farm	Water Depth	$H_{s,50}$	$T_{p,50}$
Barrow II	18	7.5	9.7
Belwind IV	20	8.4	10.3
Walney I	21.5	9	10.6
London Array 1	25	10.5	11.5
Thanet III	27	11.3	11.9

As turbine technologies are advancing, it is important to know the extreme loads acting on the larger turbines, which might have an impact on their design. In this study, IEA 15 MW is considered as part of the case study. A comparison of the extreme loads between the simplified and OpenFAST methods is shown in Figures 7 and 8 for the ETM with the 50-year EWH and the EOG with the 1-year EWH, respectively. It can be seen that as the water depth increases, there is an increase in extreme loads for both loading conditions. Further, it can be observed that for higher water depths, the simplified method is over-conservative compared to OpenFAST. Likewise, when comparing the shear forces using the simplified and OpenFAST approaches, the differences are compared to the case when looking at the differences in the resulting bending moments. For instance, the simplified method for Barrow II shows 21.2% and 37.8% error compared to the OpenFAST approach for shear force and bending moment, respectively, corresponding to the ETM with the 50 year EWH, while, for the EOG with the 1 year EWH showed percentage errors of 41.7% and 54.7%. Similarly, for Thanet III, the shear forces detected using the simplified method were 29.9% and 35.6%, while we obtained bending moments of 46.6% and 51.7% compared to the OpenFAST results corresponding to the ETM with the 50 year EWH and the EOG with the 1 year EWH, respectively. This suggests that the simplified method is more conservative than the OpenFAST approach. It can be concluded that the approach for load cases and the resulting mudline loads using the simplified method can be used for initial pile design at the preliminary stage of the typical monopile design. However, factors of 1.5 and 2 may be used for the shear force and bending moment, respectively, to simplified method results to approximately match OpenFAST results, which can be considered in the design. The factors 1.5 and 2 are obtained based on the ratio of simplified-to-OpenFAST results across all sites considered in this study. For example, loads from simplified results divided by the respective factors will yield approximate loads corresponding to the OpenFAST results.

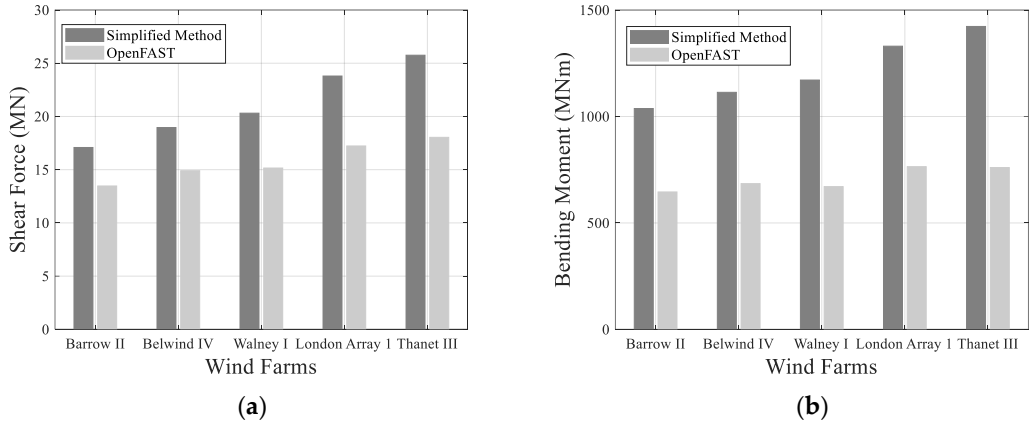

Figure 7. Comparison of extreme loads at mudline for ETM with 50 year EWH: (**a**) shear force; (**b**) bending moment.

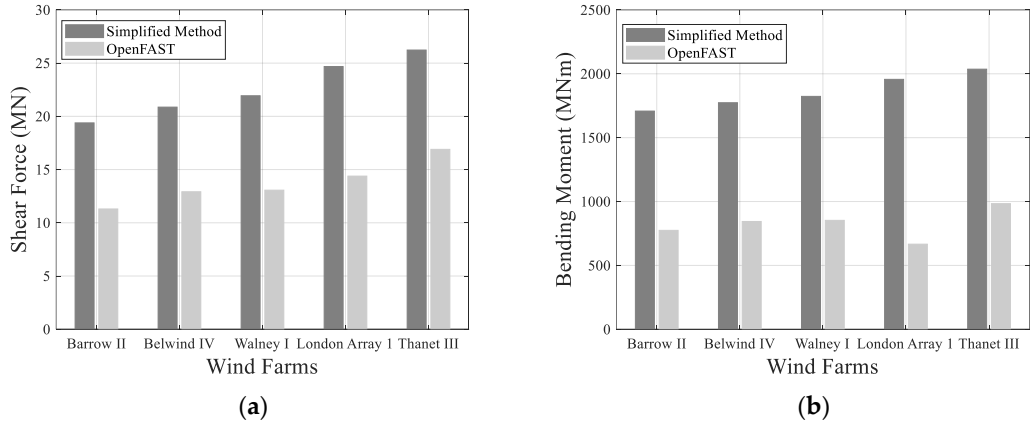

Figure 8. Comparison of extreme loads at mudline for EOG with 1 year EWH: (**a**) shear force; (**b**) bending moment.

4.4. Pile Penetration Length

In general, soil reaction curves are required to calculate the pile embedment length. These soil reaction curves are normally generated using the API method [52]. However, the API method is based on the smaller piles with an L/D ratio of 34.4, while the currently installed monopile has an L/D ratio of less than 10 [7,53]. Thus, in this study, PISA-based soil reaction curves are used when this method is appropriate for the larger diameter of the monopiles [54]. In addition to soil reaction curves, the pile penetration length is chosen when the influence of an increase in length will not have much impact on the rotation and displacement at the mudline level under Ultimate Limit State (ULS) and Serviceability Limit State (SLS) conditions. To achieve this, the following criteria should be satisfied:

- For the serviceability limit state, DNVGL [50] requires the prediction of the accumulation of permanent pile rotation at the mudline as a function of the SLS loading condition. In this study, the limit considered is 0.5 degrees [23,46]. The pile penetration length will be increased until the criteria are satisfied for corresponding loads and soil conditions.
- DNVGL [50] clause 7.6.2.5 states the necessity of verification through safety analysis. The partial safety factor under ULS should be less than the material factor of 1.25.
- DNVGL [50] clause 7.6.2.5 states that the maximum pile head deflection at the mudline should be less than the specified limit under ULS loading conditions. In this study, the limit considered is 0.5 m [46]. The pile penetration length will be increased until the rotation is below 0.5 m for the corresponding loads and soil conditions.

- The maximum pile head rotation at the mudline should be less than 1.5 degrees under ULS loading conditions [55].
- The natural frequency of the system should be greater than 1P + 10% where 1P for the IEA 15 MW is 0.126 Hz. Hence, the resulting natural frequency of the system should be greater than 0.138 Hz.

The mudline loads obtained in the previous section are used here for the calculation of the pile embedment length, which should satisfy the criteria described above. Further, in this study, medium-dense sand with a unit weight of 19 kN/m^3 and a relative density of 50% (API 2014) is considered, to investigate the change in the pile penetration length for the considered wind farms. The results for the pile penetration lengths are shown in Figure 9. These are based on the mudline loads obtained in Section 4.3 but consider the factors of 1.5 and 2 for shear forces and bending moments, respectively, in the simplified method. Figure 9 shows the pile embedment lengths for each site following the criteria stated above between two methods corresponding to medium-dense sand conditions. It can be observed that the pile penetrations obtained from the two methods are in a similar range. This shows that the use of factors in the simplified method is appropriate to use as part of the preliminary design of monopiles, as opposed to using time-consuming methods. The use of the factors enables the simple and easy determination of the loads and design of foundation structures without the need for complex and detailed analysis methods. This can be particularly useful in the initial stages of the design process, where a quick and rough estimate of the foundation loads and design is needed. However, it is important to note that the simplified method may not be appropriate for more advanced or detailed design stages, where a more thorough analysis is required.

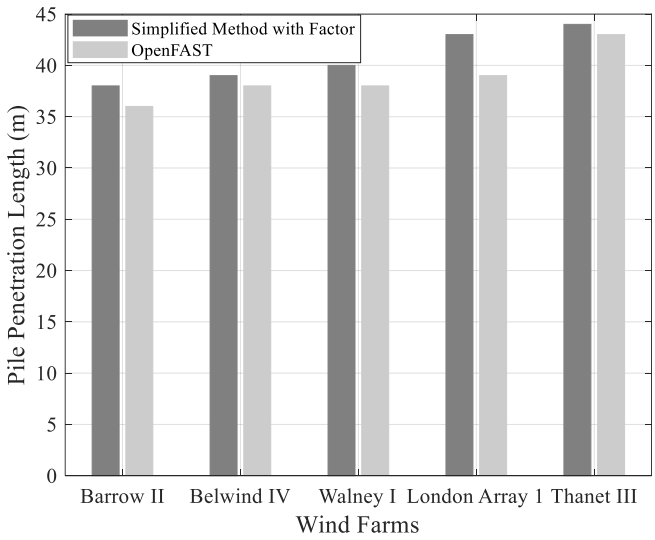

Figure 9. Comparison of pile penetration lengths between simplified method with factor and OpenFAST method for five different wind farms.

5. Conclusions

This paper presents a comparison of the loads estimated for OWTs supported on monopile foundations using a simplified and OpenFAST method for three different reference turbines, including NREL 5 MW, DTU 10 MW, and IEA 15 MW. The mudline loads corresponding to the scenarios of the ETM with a 50-year EWH and the EOG with a 1-year EWH are obtained for each case. It can be concluded from the comparison that the simplified method results in higher mudline loads compared to the OpenFAST results. In addition, the different case studies against the IEA 15 MW turbine show that the higher water depth leads to higher loads at the mudline. Therefore, the results suggest that factors of 1.5 and 2 may be used for the shear force and bending moment, respectively, to approximately match the results from OpenFAST during the early design phase of monopile foundations and

during the tendering phase. This study also provides the results for pile penetration lengths using mudline loads from OpenFAST and a simplified method with factors corresponding to different water depths for IEA 15 MW. It can be concluded that if the pile penetration length is calculated using the loads with the suggested scaling factor, then it would result in a similar length to that calculated via OpenFAST. However, the results from the simplified approach do not imply the detailed design loads. In addition, it should be noted that in this study, the IEA 15 MW is considered, which is the largest reference turbine. As larger turbines are expected to be deployed in the coming years, the current study can provide useful insights into the behaviour of larger turbines under operational loads. In particular, this should be considered when researchers derive representative scaling rules for them.

Author Contributions: Conceptualization, S.B., A.M. and S.J. (Satish Jawalageri); Methodology, S.J. (Satish Jawalageri) and A.M.; Software, S.J. (Satish Jawalageri); Validation, S.J. (Satish Jawalageri); Formal analysis, S.J. (Satish Jawalageri); Investigation, S.J. (Satish Jawalageri); Writing—original draft, S.J. (Satish Jawalageri); Writing—review & editing, S.B., S.J. (Soroosh Jalilvand) and A.M.; Supervision, S.J. (Soroosh Jalilvand) and A.M.; Funding acquisition, A.M. All authors have read and agreed to the published version of the manuscript.

Funding: Financial support received from the Irish Research Council (IRC) EBPPG/2020/259.

Data Availability Statement: The original contributions presented in the study are included in the article, further inquiries can be directed to the corresponding author. The raw data supporting the conclusions of this article will be made available by the authors on request.

Acknowledgments: The authors are grateful to Jason Jonkman from National Renewable Energy Laboratory (NREL) for his support with OpenFAST software. The authors wish to express their gratitude for the financial support received from the Irish Research Council (IRC).

Conflicts of Interest: Authors Satish Jawalageri and Soroosh Jalilvand were employed by the company Gavin and Doherty Geosolutions. The remaining authors declare that the research was conducted in the absence of any commercial or financial relationships that could be construed as a potential conflict of interest.

Nomenclature

PSD	power spectral density
DLCs	design load cases
ETM	Extreme Turbulence Model
EOG	Extreme Operating Gust
ULS	Ultimate Limit State
I_{ref}	reference turbulence intensity
U_{avg}	long-term average wind speed
U_R	rated wind speed
u_{ETM}	maximum turbulent wind speed component
L_k	integral length scale
$f_{1P,max}$	rotational speed of the turbine
$F_{wind,ETM}$	lateral force at the mudline
$M_{wind,ETM}$	moment at the mudline
ρ_a	density of air
A_R	rotor-swept area
C_T	thrust coefficient
S	water depth
z_{hub}	hub height above sea level
u_{EOG}	maximum wind speed component of EOG condition
H_1	Extreme Wave Height corresponding to return period of 1 year
$H_{S,50}$	Extreme Wave Height corresponding to return period of 50 year

$F_{D,max}$	maximum drag forces
$F_{I,max}$	maximum inertia forces
$M_{D,max}$	maximum drag moments
$M_{I,max}$	maximum inertia moments
C_D	drag coefficients
C_m	inertia coefficients
η	surface elevation
$V(z)$	mean wind speed at the height z above the MSL
V_{hub}	mean wind speed at hub height
$D\ dz$	area of the strip with diameter (D)
$A(z)dz$	displaced volume
v_r	relative water velocity
SWL	still water level
$V_{OpenFAST}$	loads from OpenFAST
$V_{Simplified}$	loads obtained from the simplified method

References

1. WindEurope. *Offshore Wind in Europe, Key Trends and Statistics 2020*; WindEurope: Brussels, Belgium, 2021.
2. Malekjafarian, A.; Jalilvand, S.; Doherty, P.; Igoe, D. Foundation damping for monopile supported offshore wind turbines: A review. *Mar. Struct.* **2021**, *77*, 102937. [CrossRef]
3. Kallehave, D.; Byrne, B.W.; Thilsted, C.L.; Mikkelsen, K.K. Optimization of monopiles for offshore wind turbines. *Philos. Trans. R. Soc. A Math. Phys. Eng. Sci.* **2015**, *373*, 20140100. [CrossRef] [PubMed]
4. Prendergast, L.J.; Reale, C.; Gavin, K. Probabilistic examination of the change in eigenfrequencies of an offshore wind turbine under progressive scour incorporating soil spatial variability. *Mar. Struct.* **2018**, *57*, 87–104. [CrossRef]
5. Reale, C.; Tott-Buswell, J.; Prendergast, L.J. Impact of Geotechnical Uncertainty on the Preliminary Design of Monopiles Supporting Offshore Wind Turbines. *ASCE-ASME J. Risk Uncertain. Eng. Syst. Part B Mech. Eng.* **2021**, *7*, 040903. [CrossRef]
6. WindEurope. *Offshore Wind Energy 2022 Statistics 2023*; WindEurope: Brussels, Belgium, 2023.
7. Krolis, V.D.; van der Zwaag, G.L.; de Vries, W. Determining the Embedded Pile Length for Large-Diameter Monopiles. *Mar. Technol. Soc. J.* **2010**, *44*, 24–31. [CrossRef]
8. Qi, W.G.; Gao, F.P.; Randolph, M.F.; Lehane, B.M.; Amini, S.A.; Mohammad, T.A.; Aziz, A.A.; Ghazali, A.H.; Huat, B.B.K.; Day, R.A.; et al. Scour effects on p–y curves for shallowly embedded piles in sand. *Géotechnique* **2016**, *66*, 648–660. [CrossRef]
9. Jia, X.; Zhang, H.; Wang, C.; Liang, F.; Chen, X. Influence on the lateral response of offshore pile foundations of an asymmetric heart-shaped scour hole. *Appl. Ocean Res.* **2023**, *133*, 103485. [CrossRef]
10. Sørensen, S.P.H.; Ibsen, L.B. Assessment of foundation design for offshore monopiles unprotected against scour. *Ocean Eng.* **2013**, *63*, 17–25. [CrossRef]
11. Prendergast, L.J.; Gavin, K.; Doherty, P. An investigation into the effect of scour on the natural frequency of an offshore wind turbine. *Ocean Eng.* **2015**, *101*, 1–11. [CrossRef]
12. Wu, C.; Wang, Q.; Luo, K.; Fan, J. Mesoscale impact of the sea surface on the performance of offshore wind farms. *J. Clean. Prod.* **2022**, *372*, 133741. [CrossRef]
13. Pettas, V.; Kretschmer, M.; Clifton, A.; Cheng, P.W. On the effects of inter-farm interactions at the offshore wind farm Alpha Ventus. *Wind Energy Sci.* **2021**, *6*, 1455–1472. [CrossRef]
14. Bhattacharya, S. *Design of Foundations for Offshore Wind Turbines*; John Wiley & Sons Ltd.: Hoboken, NJ, USA, 2019.
15. Jacomet, A.; Khosravifardshirazi, A.; Sahafnejad-Mohammadi, I.; Dibaj, M.; Javadi, A.A.; Akrami, M. Analysing the Influential Parameters on the Monopile Foundation of an Offshore Wind Turbine. *Computation* **2021**, *9*, 71. [CrossRef]
16. Chew, K.-H.; Tai, K.; Ng, E.Y.K.; Muskulus, M. Optimization of Offshore Wind Turbine Support Structures Using an Analytical Gradient-based Method. *Energy Procedia* **2015**, *80*, 100–107. [CrossRef]
17. Wang, S.; Larsen, T.J.; Bredmose, H. Ultimate load analysis of a 10 MW offshore monopile wind turbine incorporating fully nonlinear irregular wave kinematics. *Mar. Struct.* **2021**, *76*, 102922. [CrossRef]
18. Bhattacharya, S. Challenges in Design of Foundations for Offshore Wind Turbines. *Eng. Technol. Ref.* **2014**, *1*, 922. [CrossRef]
19. Schløer, S.; Castillo, L.G.; Fejerskov, M.; Stroescu, E.; Bredmose, H. A model for Quick Load Analysis for monopile-type offshore wind turbine substructures. *Wind Energ. Sci.* **2016**, *3*, 57–73. [CrossRef]
20. Jeong, Y.-J.; Park, M.-S.; Kim, J.; Song, S.-H. Wave Force Characteristics of Large-Sized Offshore Wind Support Structures to Sea Levels and Wave Conditions. *Appl. Sci.* **2019**, *9*, 1855. [CrossRef]
21. He, K.; Ye, J. Dynamics of offshore wind turbine-seabed foundation under hydrodynamic and aerodynamic loads: A coupled numerical way. *Renew. Energy* **2023**, *202*, 453–469. [CrossRef]
22. Abdullahi, A.; Bhattacharya, S.; Li, C.; Xiao, Y.; Wang, Y. Long-term effect of operating loads on large monopile-supported offshore wind turbines in sand. *Ocean Eng.* **2022**, *245*, 110404. [CrossRef]

23. Bisoi, S.; Haldar, S. Dynamic analysis of offshore wind turbine in clay considering soil–monopile–tower interaction. *Soil Dyn. Earthq. Eng.* **2014**, *63*, 19–35. [CrossRef]
24. Jawalageri, S.; Prendergast, L.J.; Jalilvand, S.; Malekjafarian, A. Effect of scour erosion on mode shapes of a 5 MW monopile-supported offshore wind turbine. *Ocean Eng.* **2022**, *266*, 113131. [CrossRef]
25. Teixeira, R.; Nogal, M.; O'Connor, A.; Nichols, J.; Dumas, A. Stress-cycle fatigue design with Kriging applied to offshore wind turbines. *Int. J. Fatigue* **2019**, *125*, 454–467. [CrossRef]
26. Løken, I.B.; Kaynia, A.M. Effect of foundation type and modelling on dynamic response and fatigue of offshore wind turbines. *Wind Energy* **2019**, *22*, 1667–1683. [CrossRef]
27. Abhinav, K.A.; Saha, N.; Cox, J.A.; Bhattacharya, S.; Nanda, S.; Arthur, I.; Sivakumar, V.; Donohue, S.; Bradshaw, A.; Keltai, R.; et al. Dynamic analysis of monopile supported offshore wind turbines. *Proc. Inst. Civ. Eng. Geotech. Eng.* **2017**, *170*, 428–444. [CrossRef]
28. *IEC 61400-3-1:2019&A11:2020*; Wind Energy Generation Systems—Part 3-1: Design Requirements for Fixed Offshore Wind Turbines. IEC: Geneva, Switzerland, 2020.
29. *DNVGL-ST-0437*; Loads and Site Conditions for Wind Turbines. DNV GL: Høvik, Norway, 2016.
30. Van Der Tempel, J. Design of Support Structures for Offshore Wind Turbines. Ph.D. Thesis, Delft University of Technology, Delft, The Netherlands, 2006.
31. Muskulus, M.; Schafhirt, S. Design Optimization of Wind Turbine Support Structures—A Review. *J. Ocean Wind Energy* **2014**, *1*, 12–22.
32. Chen, I.W.; Wong, B.-L.; Lin, Y.-H.; Chau, S.-W.; Huang, H.-H. Design and Analysis of Jacket Substructures for Offshore Wind Turbines. *Energies* **2016**, *9*, 264. [CrossRef]
33. Srikanth, I.; Alluri, S.K.R.; Balakrishnan, K.; Murthy, M.V.R.; Arockiasamy, M. Simplified Design Procedure of Monopile Foundation for Offshore Wind Turbine in Gujarat, India. *J. Shipp. Ocean Eng.* **2017**, *4*, 133–152.
34. Yang, C.; Wang, R.; Zhang, J. A simplified method for analyzing the fundamental frequency of monopile supported offshore wind turbine system design. *Earthq. Eng. Eng. Vib.* **2018**, *17*, 893–901. [CrossRef]
35. Ma, H.; Chang, X.; Deng, Y.; Yang, J. A simplified method for estimating the permanent accumulated rotation of an offshore wind turbine monopile throughout its design life. *Ocean Eng.* **2022**, *265*, 112664. [CrossRef]
36. Li, X.-j.; Dai, G.-l.; Zhu, M.-x.; Wang, L.-y.; Liu, H.-y. A Simplified Method for Estimating the Initial Stiffness of Monopile—Soil Interaction Under Lateral Loads in Offshore Wind Turbine Systems. *China Ocean Eng.* **2023**, *37*, 165–174. [CrossRef]
37. Arany, L.; Bhattacharya, S.; Macdonald, J.; Hogan, S.J. Design of monopiles for offshore wind turbines in 10 steps. *Soil Dyn. Earthq. Eng.* **2017**, *92*, 126–152. [CrossRef]
38. IEC. *International Standard IEC-61400-1 Wind Turbines—Part 1: Design Requirements*, 3rd ed.; IEC: Geneva, Switzerland, 2005.
39. Liang, F.; Yuan, Z.; Liang, X.; Zhang, H. Seismic response of monopile-supported offshore wind turbines under combined wind, wave and hydrodynamic loads at scoured sites. *Comput. Geotech.* **2022**, *144*, 104640. [CrossRef]
40. *NREL/TP-500-36881*; AeroDyn Theory Manual. National Renewable Energy Laboratory: Golden, CO, USA, 2005.
41. *DNV-RP-C205*; Environmental Conditions and Environmental Loads. DNV GL: Høvik, Norway, 2014.
42. Jonkman, J.M.; Robertson, A.N.; Hayman, G.J. *HydroDyn User's Guide and Theory Manual*; National Renewable Energy Laboratory: Golden, CO, USA, 2016.
43. Morison, J.R.; Johnson, J.W.; Schaaf, S.A. The force exerted by surface waves on piles. *J. Pet. Technol.* **1950**, *2*, 149–154. [CrossRef]
44. Damiani, R.; Jonkman, J.; Hayman, G. *SubDyn User's Guide and Theory Manual*; National Renewable Energy Laboratory: Golden, CO, USA, 2015.
45. Jonkman, J.; Jonkman, B. *OpenFAST Manual*; National Renewable Energy Laboratory: Golden, CO, USA, 2020.
46. Jalbi, S.; Arany, L.; Salem, A.; Cui, L.; Bhattacharya, S. A method to predict the cyclic loading profiles (one-way or two-way) for monopile supported offshore wind turbines. *Mar. Struct.* **2019**, *63*, 65–83. [CrossRef]
47. Jonkman, J.; Butterfield, S.; Musial, W.; Scott, G. *Definition of a 5-MW Reference Wind Turbine for Offshore System Development*; National Renewable Energy Laboratory: Golden, CO, USA, 2009.
48. Bak, C.; Zahle, F.; Bitsche, R.; Kim, T.; Yde, A.; Henriksen, L.C.; Hansen, M.H.; Blasques, J.P.A.A.; Gaunaa, M.; Natarajan, A. The DTU 10-MW Reference Wind Turbine, Danish Wind Power Research, Trinity. In Proceedings of the Danish Wind Power Research 2013, Fredericia, Denmark, 27–28 May 2013.
49. Gaertner, E.; Rinker, J.; Sethuraman, L.; Zahle, F.; Anderson, B.; Barter, G.; Abbas, N.; Meng, F.; Bortolotti, P.; Skrzypinski, W.; et al. *Definition of the IEA Wind 15-Megawatt Offshore Reference Wind Turbine*; National Renewable Energy Laboratory: Golden, CO, USA, 2020.
50. *DNV-ST-0126*; Support Structures for Wind Turbines. DNV GL: Høvik, Norway, 2016.
51. Leblanc, C.; Houlsby, G.T.; Byrne, B.W. Response of stiff piles in sand to long-term cyclic lateral loading. *Géotechnique* **2010**, *60*, 79–90. [CrossRef]
52. API. *Geotechnical and Foundation Design Considerations*; API: Washington, DC, USA, 2014.
53. Velarde, J.; Bachynski, E.E. Design and fatigue analysis of monopile foundations to support the DTU 10 MW offshore wind turbine. *Energy Procedia* **2017**, *137*, 3–13. [CrossRef]

54. Berthelot, P.; Byrne, B.W.; Burd, H.J.; Zdravković, L.; McAdam, R.A.; Taborda, D.M.G.; Houlsby, G.T.; Jardine, R.J.; Martin, C.M.; Potts, D.M.; et al. PISA: New design methods for offshore wind turbine monopiles. *Rev. Fr. Geotech.* **2019**, *158*, 3.
55. Fitzgerald, B.; Igoe, D.; Sarkar, S. A Comparison of Soil Structure Interaction Models for Dynamic Analysis of Offshore Wind Turbines. *J. Phys. Conf. Ser.* **2020**, *1618*, 052043. [CrossRef]

Disclaimer/Publisher's Note: The statements, opinions and data contained in all publications are solely those of the individual author(s) and contributor(s) and not of MDPI and/or the editor(s). MDPI and/or the editor(s) disclaim responsibility for any injury to people or property resulting from any ideas, methods, instructions or products referred to in the content.